Structural and functional characterisation of ferret interleukin-2

Bin Ren [a], William J. McKinstry [a], Tam Pham [a], Janet Newman [a], Daniel S. Layton [b], Andrew G. Bean [b], Zhenjun Chen [c], Karen L. Laurie [d], Kathryn Borg [d], Ian G. Barr [d], Timothy E. Adams [a, *]

[a] CSIRO Manufacturing, Parkville, VIC 3052, Australia
[b] CSIRO Health and Biosecurity, Geelong, VIC 3219, Australia
[c] Department of Microbiology and Immunology, The University of Melbourne at the Doherty Institute, Melbourne, VIC 3000, Australia
[d] WHO Collaborating Centre for Reference and Research on Influenza (VIDRL), Peter Doherty Institute for Infection & Immunity, Melbourne, Australia

ARTICLE INFO

ABSTRACT

While the ferret is a valuable animal model for a number of human viral infections, such as influenza, Hendra and Nipah, evaluating the cellular immune response following infection has been hampered by the lack of a number of species-specific immunological reagents. Interleukin 2 (IL-2) is one such key cytokine. Ferret recombinant IL-2 incorporating a C-terminal histidine tag was expressed and purified and the three-dimensional structure solved and refined at 1.89 Å by X-ray crystallography, which represents the highest resolution and first non-human IL-2 structure. While ferret IL-2 displays the classic cytokine fold of the four-helix bundle structure, conformational flexibility was observed at the second helix and its neighbouring region in the bundle, which may result in the disruption of the spatial arrangement of residues involved in receptor binding interactions, implicating subtle differences between ferret and human IL-2 when initiating biological functions. Ferret recombinant IL-2 stimulated the proliferation of ferret lymph node cells and induced the expression of mRNA for IFN-γ and Granzyme A.

1. Introduction

Interleukin-2 (IL-2) is a pleiotropic cytokine that plays a key role in the regulation of T cell homoeostasis and self-tolerance. While mice that lack IL-2 (Il-$2^{-/-}$) are not immunosuppressed, they exhibit a number of phenotypes that point to immunological dysfunction (Schorle et al., 1991). Serum IgM levels are unaffected, but IgG$_1$ levels are suppressed >20-fold, suggesting impaired CD4$^+$ T cell helper function, despite no overt change in the profile of the major T cell compartments in the thymus and peripheral lymphoid tissues. Similarly, Il-$2^{-/-}$ mice recover from infection with lymphocytic choriomeningitis virus (LCMV) despite a significant reduction (up to 90%) in the generation of virus-specific cytotoxic CD8$^+$ T cells (Cousens et al., 1995; Kundig et al., 1993). However, the absence of IL-2 results in the inability to mount an effective secondary response, a reflection of the failure of memory cell expansion upon challenge (D'Souza and Lefrancois, 2003; Williams et al., 2006). Paradoxically, over time, a lack of IL-2 is associated with the development of a fatal, multi-organ autoimmune disease, characterised by the polyclonal activation of B and T cells, and the production of autoantibodies (Sadlack et al., 1995, 1993). This lack of immunological self-tolerance has been identified as being caused by the absence of CD4$^+$ CD25$^+$ regulatory T cells, the development of which is IL-2-dependent (Almeida et al., 2002; Malek et al., 2002; Papiernik et al., 1998). Collectively, these and many other studies have elucidated the pivotal role played by IL-2 in regulating both the effector and regulatory arms of T cell biology (Boyman and Sprent, 2012).

The primary source of IL-2 is activated CD4$^+$ T cells, although a variety of other cell types including dendritic, mast and CD8$^+$ T cells may secrete IL-2 in response to different stimuli (Boyman and Sprent, 2012). The high-affinity cell-surface receptor for IL-2 comprises three proteins — IL-2Rα (CD25), IL-2Rβ(CD122) and the common γ-chain (γ-$_c$ or CD132) — and is expressed on antigen-activated and regulatory T cells (Malek and Castro, 2010). The receptor subunits IL-2Rβ and γ-$_c$ can form a dimer that binds IL-2 with moderate affinity and signal in the absence of the IL-2Rα

subunit (Boyman et al., 2006); nonetheless, the high-affinity, trimeric receptor complex is essential for the development of T cell homoeostasis *in vivo*, as mice that lack the IL-2Rα subunit are phenotypically indistinguishable from IL-2-deficient mice (Willerford et al., 1995). The sequential assembly of the functional ligand-receptor signalling complex has been elucidated at a structural level, with the initial formation of an IL-2:IL-2Rα dimer providing a discrete interface for the recruitment of the IL-2Rβ subunit, with no contact being made between the respective receptor partners (Stauber et al., 2006; Wang et al., 2005). Within this trimeric complex, IL-2 and IL-2Rβ provide a composite interface for the recruitment of the γ-c receptor. At a cellular level, the formation of the quaternary signalling complex results in the activation of two members of the JAK family of tyrosine kinases, JAK1 and JAK3, and signal transduction via a number of canonical pathways (Boyman and Sprent, 2012).

Despite the importance of the ferret as a disease model for pathogenic human viruses that includes influenza, severe acute respiratory coronavirus (SARS-CoV) (Cameron et al., 2012), Hendra virus (Pallister et al., 2011) and Nipah virus (Bossart et al., 2009), ferret-specific reagents to monitor and investigate the immune response are lacking. Only a handful of cell-surface markers for different cell types are available (Music et al., 2014), while the quantitation of immune cytokines is determined only by their relative mRNA levels rather than protein levels (Carolan et al., 2014). There is virtually no information on the use of ferret-specific or ferret cross-reactive growth additives or differentiation factors for ferret cell culture. With the recent publication of the ferret genome (Peng et al., 2014) it is hoped that the flow of reagents will increase so that much more sophisticated studies can be undertaken to follow or prevent infection. Here we describe the expression, activity and crystal structure of ferret recombinant IL-2 and show that while it has similarities to human IL-2, it retains some unique features that presumably have evolved with the species.

2. Materials and methods

2.1. Animals

Ferret lymph nodes were taken from 3 to 12 month old ferrets aseptically in accordance with CSIRO Australian Animal Health Laboratories animal ethics approval. Additional experiments were conducted with approval from the CSL Limited/Pfizer Animal Ethics Committee, in accordance with the NHMRC Australian code of practice for the care and use of animals for scientific purposes.

2.2. Vector assembly

A DNA template encoding the complete ferret IL-2 coding region (amino acid residues 1–152; UniProtKB-A3FBE6), optimised for expression in human cell lines, was obtained from GenScript (Piscataway, USA). A C-terminal hexahistidine tag was included to facilitate purification. The coding region insert was isolated and sub-cloned into the mammalian expression vector, pCAGGS, and plasmid DNA prepared from transformed bacterial host cells using a Maxiprep kit (Qiagen, Hilden, Germany).

2.3. Cell culture, transient transfection and purification of ferret recombinant IL-2

Suspension-adapted cultures of FreeStyle™-293 cells (Life Technologies, Carlsbad, USA) were grown in Freestyle 293 Expression Medium (Life Technologies) supplemented with Glutamax™-I. Scale-up transient transfection was performed on a one litre culture of FreeStyle™-293 cells (2×10^6 per ml) in a three litre flask using linear polyethylenimine (PEI, Polysciences, Inc., Warrington, USA) according to a published protocol (Tom et al., 2008). The culture was harvested after seven days (cell viability ~50%), clarified by centrifugation and filtered. Recombinant IL-2 was purified from 1.6 L of conditioned medium by immobilized metal ion affinity chromatography (IMAC; 5 mL HisTRAP HP column, GE Healthcare, Little Chalfont, UK) followed by gel filtration chromatography on a Superdex 75 16/60 column (GE Healthcare) equilibrated in phosphate-buffered saline (PBS) under conditions to minimise endotoxin contamination. Endotoxin levels were measured by the Endosafe–PTS assay (Charles River, USA) and were of the order of 1.90 units/mg of protein.

The purification of recombinant ferret IL-2 was monitored by SDS-PAGE under both non-reducing and reducing conditions on a 4–12% Bis-Tris NuPAGE gel (Life Technologies) using MES-SDS electrophoresis buffer. Samples were incubated with SDS sample buffer either in the presence or absence of 10 mM 1,4-dithiothreitol as reducing agent, and heated to 95 °C for 5 min prior to loading onto gels. Protein gels were stained with Coomassie Brilliant Blue.

2.4. Crystallization

Initial crystallization conditions were screened at both 8 °C and 20 °C using the "1-Click Screening strategy" at the CSIRO Collaborative Crystallisation Centre (C3), Melbourne, Australia (crystal. csiro.au). Sitting drops of 300 nL were set up using a Phoenix robot (Art Robbins Industries, Sunnyvale, USA). The droplet was a mixture of the protein and reservoir solution with a volume ratio of 1:1 or 2:1, which was equilibrated against 50 μL reservoir solution in 96-well plates (IDEX Corporation, Lake Forrest, USA). The protein concentration was 15 mg mL^{-1}, based on the result from the Pre-Crystallization Test (Hampton Research, Aliso Viejo, USA). Crystals began to emerge rapidly within one hour or one day in a number of conditions with lithium sulfate or ammonium sulfate as the major precipitant and citrate solutions as the buffer. Well-diffracting crystals were obtained from a droplet at 20 °C containing the reservoir solution 0.8 M ammonium sulfate and 0.1 M sodium citrate - citric acid buffer at pH 4.0. The crystals reached a maximum dimension of ~200 μm within 3 days. Larger crystals with a maximum dimension of about 500 μm were obtained from larger sitting drops set up in a 24-well Cryschem plate (Hampton Research). Each droplet had a volume of 4 μL, which was an equal volume mixture of the protein and reservoir solution, and was equilibrated against 500 μL reservoir solution.

2.5. X-ray diffraction

Diffraction data were collected at −173 °C on the MX1 beamline at the Australian Synchrotron (Melbourne, Australia) using the ADSC Quantum 210r detector. The reservoir solution, supplemented by the addition of 20% (v/v) PEG 200, was used as cryoprotectant. The data set consisted of 180 images of 1° oscillation diffraction collected at a wavelength of 0.9537 Å and distance of 150 mm. The data were processed with the program XDS (Kabsch, 2010). The obtained *hkl* intensities were input into the *CCP*4 program package for Laue symmetry examination, intensity scaling and reduction (Winn et al., 2011). The crystal was found to belong to the one of the enantiomorphic space groups $P3_121$ or $P3_221$ with cell dimensions of $a = b = 92.9$ Å, $c = 89.3$ Å, and $\alpha = \beta = 90°$, $\gamma = 120°$. The processed data set was complete to the resolution of 1.89 Å (Table 1).

2.6. Structure determination and refinement

The structure was solved by molecular replacement with Phaser

Table 1
Diffraction data and refinement statistics.

Diffraction data	
Space group	$P3_221$
a, b, c (Å)	92.9, 92.9, 89.3
α, β, γ (°)	90, 90, 120
Resolution (Å)	1.89 (1.94–1.89)
No. of observations	38,9181
Unique reflections	35,935
Multiplicity	10.8 (10.7)
Mean $I/\sigma(I)$	14.7 (2.8)
Completeness (%)	99.9 (98.5)
R_{merge}[a]	0.097 (0.677)
$R_{p.i.m}$[b]	0.031 (0.215)
Refinement	
R-work/R-free[c]	0.1650/0.1973
No. of copies in the asymmetric unit	2
No. of non-H atoms	2371
Average B factors (Å^2)	35.8
r.m.s.d. bond length (Å)	0.020
r.m.s.d. bond angle (°)	1.649
Ramachandran plot	
Favoured regions (%)	94.6
Allowed regions (%)	5.4
Outlier regions (%)	0.0

The values in parentheses are for the highest resolution bin.

[a] $R_{merge} = \sum |I - \langle I \rangle| / \sum I$, where I is the observation of reflection intensity and $\langle I \rangle$ is the weighted average intensity for multiple and symmetry-related measurements.

[b] Multiplicity-weighted R_{merge} from all reflections. For a definition, see Evans (2006).

[c] 5% diffraction data were set aside to calculate the free R-factor during refinement.

(McCoy et al., 2007) using the structure of human interleukin-2 (IL-2) as the search model (PDB code 1M47) (Arkin et al., 2003). The space group was determined to be $P3_221$ during structure solution. The correct solution found a dimer in the asymmetric unit with a translation function Z score (TFZ) of 7.1 (McCoy et al., 2007). Iterative model-building and refinement were carried out with Coot (Emsley et al., 2010) and Phenix (Adams et al., 2010). The final model has a R-work of 16.5% and R-free of 19.7% at 1.89 Å with no outliers in the Ramachandran plot (Table 1). It comprises two independent ferret IL-2 molecules, designated as molecule 1 (residues of 5–132) and molecule 2 (residues 6–132). In addition to the few missing residues at the N-termini, other residues that are not included in the final model due to poor electron density include Asn75 and Phe76 of molecule 1 and the residues of the C-terminal hexahistidine tag for both molecules. The final atomic coordinates and structure factors have been deposited into the RCSB Protein Data Bank with the access code 4ZF7.

2.7. Harvest of ferret lymph node (LN) cells

Whole lymph node was obtained and single cell suspensions were prepared. Lymph nodes were cleaned of any connective tissue and mechanically digested in cold PBS buffer to produce a single suspension. Mechanical digestion was achieved by pressing the lymph node through a 70 μm sieve (BD Biosciences, East Rutherford, USA) using the plunger of a 10 mL syringe. Single cell suspensions were transferred to 50 mL Falcon tubes and centrifuged for 5 min at $400 \times g$. The pellet obtained was resuspended in culture medium (DMEM, Life Technologies) supplemented with 10% foetal calf serum, 10 μM Hepes.

2.8. T cell proliferation assay and RT-PCR

The biological activity of ferret IL-2 protein was determined using a T cell proliferation assay. Ferret LN cells from three separate ferrets (2.5×10^5 cells/well) were stimulated with 2.5 μg/mL concanavalin A (Con A) in culture medium for 24 h at 37 °C in 96-well microtiter plates. Ferret IL-2 was added at different concentration as well as the inclusion of a no IL-2 control. After 24 h the cultures were pulsed with 1 μCi ^{3}H-thymidine for an additional 24 h before being harvested onto glass fibre filter paper by a manual cell harvester. The fibre filter papers were dried and radioactivity measured using a Wallac β counter (Perkin–Elmer, Melbourne, Australia).

Ferret LN cells were cultured as previously described (Carolan et al., 2014) with the medium supplemented with 50 uM 2-
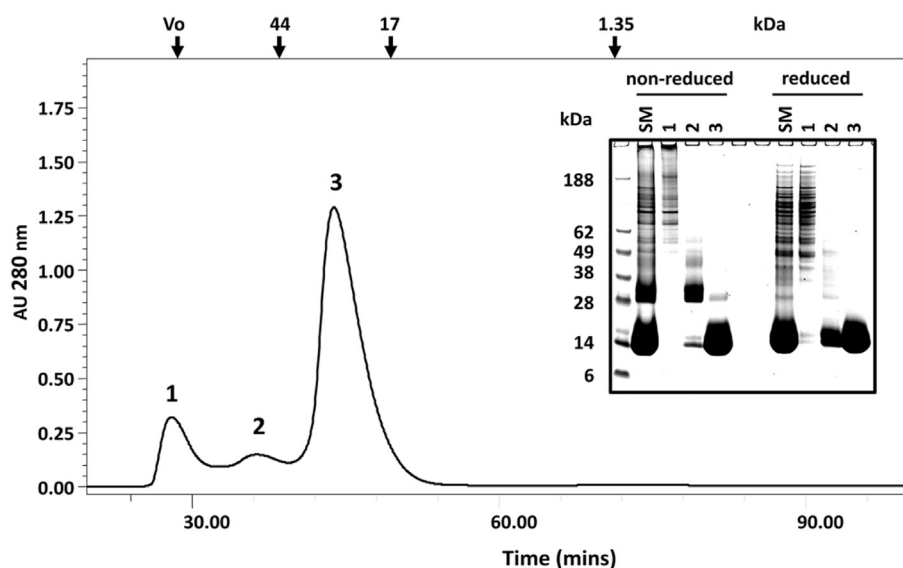

Fig. 1. Size exclusion chromatography of purified ferret recombinant IL-2. Recombinant IL-2 was recovered by IMAC and fractionated on a Superdex 75 16/60 column. The column had previously been calibrated with BioRad gel filtration standards (chicken ovalbumin, 44 kDa; horse myoglobin, 17 kDa; and vitamin B12, 1.35 kDa). SDS-PAGE analysis (4–12% Bis-Tris NuPAGE) of peak fractions under both non-reduced and reduced conditions revealed: peak 1 contained high molecular weight host cell proteins; peak 2 – covalently-associated IL-2 dimer; and peak 3 – monomeric IL-2. Abbreviations: MW, molecular weight standards; SM, starting material; kDa, kilodalton; Vo, column void volume.

mercaptoethanol. LN cells (4×10^5) were stimulated with human recombinant IL-2 (Roche Diagnostics GmbH, Basel, Switzerland) or ferret IL-2 (monomer or dimer) at various concentrations ranging from 10 to 0.0001 µg/mL (0.1 µg/mL human rIL-2 is equivalent to 200 U/ml activity) for 72 h at 37 °C, 5% CO_2. All stimulation assays were cultured in 96-well round bottom plates in a total volume of 200 µL. Cells were collected, supernatant removed and RNA extracted, cDNA prepared and the expression of Granzyme A and IFNγ mRNAs detected by real-time PCR assays as previously described (Carolan et al., 2014).

2.9. IL-2 ELISA

Two commercially available IL-2 enzyme-linked immunoassays (ELISA), the IL-2 high sensitivity human ELISA kit (Abcam, Cambridge, UK) and the mouse IL-2 ELISA (BD OptEIA, East Rutherford, USA), were tested for their reactivity against ferret IL-2. Serial dilutions (ten-fold) of ferret IL-2 monomer and multimer preparations were tested in these kits according to the manufacturer's instructions.
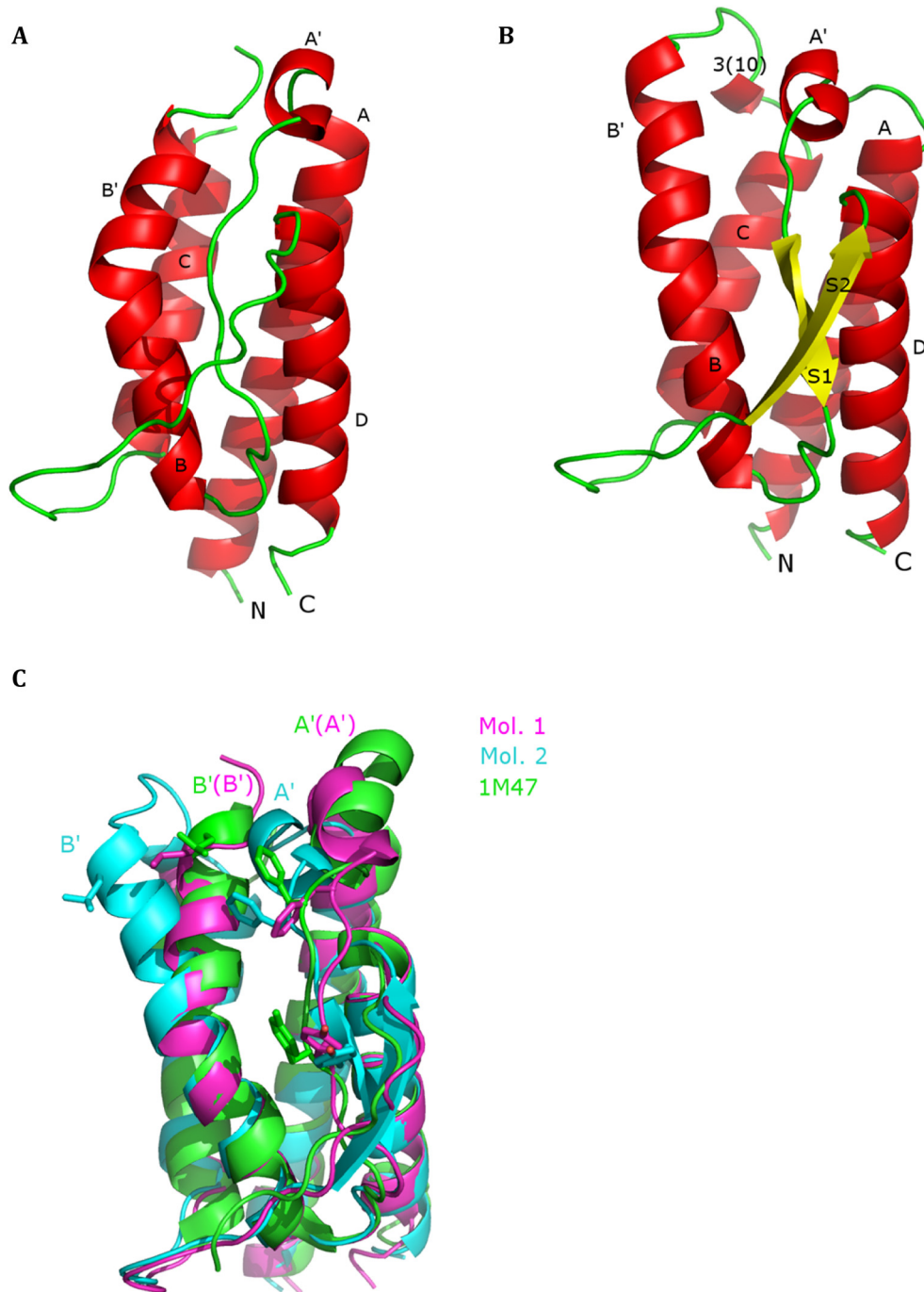

Fig. 2. Ferret IL-2 crystal structure. (A) Molecule 1 of ferret IL-2. (B) Molecule 2 of ferret IL-2. (C) Superposition of the two ferret IL-2 molecules with human IL-2 (PDB code 1M47) (Arkin et al., 2003). The side chains of the residues Phe42, Tyr45 and Leu72 in human IL-2 and Phe40, Tyr43 and Leu70 in ferret IL-2 are shown as sticks in (C). The figures were prepared with PYMOL (The PyMOL Molecular Graphics System, Schrödinger, LLC.).

2.10. Statistics

GraphPad Prism (GraphPad Software, Inc, San Diego, USA) was used to determine whether results were statistically significant. Results were significant when a one-tailed Mann Whitney test was calculated to be p < 0.05.

3. Results and discussion

3.1. Cloning, expression and purification of ferret recombinant IL-2

Ferret recombinant IL-2 containing a C-terminal hexahistidine tag, assembled in the mammalian expression vector pCAGGS, was successfully expressed in mammalian HEK 293F cells using transient transfection. The protein was purified from culture supernatant using IMAC, and the peak fraction chromatographed over a Superdex 75 gel filtration column under conditions to minimise endotoxin contamination. Three peaks were observed eluting from this column; peak 1 migrated at the column void volume (>80 kDa) and contained mainly high molecular weight host cell proteins that co-purified with multimeric ferret IL-2 during IMAC; peaks 2 and 3 migrated with apparent molecular weights of ~50 kDa and ~30 kDa, respectively (Fig. 1). SDS-PAGE analysis of these peaks identified peak 2 as a covalently-associated homo-dimer of ferret IL-2, and peak 3 was monomeric ferret IL-2 which was confirmed by N-terminal amino acid sequencing, with 10 cycles giving the expected sequence of APTTSSSTK (data not shown). Under reducing conditions, monomeric ferret IL-2 migrated as a broad band adjacent to the 14 kDa molecular weight standard, consistent with a theoretical molecular weight of 16,056 Da for the His-tagged recombinant protein following removal of the signal peptide. While peak 3 (monomer) appeared homogeneous when analysed under reducing conditions (a trace of contaminating disulphide-linked dimer is seen under non-reducing conditions), additional non-specific, higher molecular weight protein was observed in peak 2 (dimer) in addition to IL-2 (Fig. 1). A total of 37 mg of monomeric ferret IL-2 was purified to homogeneity from a 1.6 L transient HEK 293F culture. The protein was assessed as >98% pure by SDS-PAGE analysis and had minimal endotoxin contamination (1.90 endotoxin units/mg IL-2).

3.2. The structure

The structure of ferret IL-2 was solved and refined at 1.89 Å resolution, which is the highest resolution structure solved so far for any IL-2. It is also the first non-human IL-2 structure deposited in the PDB – there are about 20 PDB entries of human IL-2 either in the unbound state or in complexes with other molecules. There were two ferret IL-2 molecules in the asymmetric unit of the crystal (Fig. 2A and B). Each copy of the IL-2 molecule adopted the classic cytokine fold of the four-helix bundle structure with the helices arranged in the up-up-down-down topology (Mott and Campbell, 1995). There are two long link regions between the helices, including the one between the first (A) and second (B) helices and the other between the third (C) and fourth (D) helices. There is a short helix (A′) in the first long link region right after helix A.

The structures of the two ferret IL-2 molecules in the asymmetric unit were in general similar to each other (Fig. 2C). Structural superposition gave a root mean square deviation of 1.38 Å for 109 corresponding Cα atoms out of a total of 126. However, notable structural re-arrangements are observed when comparing the two structures. The second helix in molecule 1 is bent in the middle so that the helix is divided into helices B and B′ (Fig. 2A). Such a bent helix is an invariable feature observed in all human IL-2 structures solved to date, no matter whether the human IL-2 is in the apo state or in complexes with the receptors (Fig. 2C) (Arkin et al., 2003; Bazan, 1992; Rickert et al., 2005; Wang et al., 2005). In contrast, in molecule 2 of the ferret IL-2 structure, helices B and B′ form one straightened helix, which results from the shifting of helix A′ towards the original position of helix B′ (Fig. 2B). Examination of the crystal structure indicates that the movement of the helix A′ was caused by the approach of helix C from a neighbouring molecule due to packing contacts in the crystal. As a result of the structural adjustment, the loop regions in the middle of the two long links in molecule 2 reorganized to form an anti-parallel two-stranded β-sheet (Fig. 2B). Superposition of the two ferret IL-2 structures onto that of human IL-2 (Arkin et al., 2003) revealed root mean square deviations of 1.66 Å for 113 Cα atoms and 1.90 Å for 102 Cα atoms, for molecule 1 and 2, respectively, corroborating that the structure of molecule 1 is more similar to that of human IL-2 (Fig. 2C).

It has been suggested that the kink of the second helix of human IL-2 is caused by the proline residue Pro65 (Brandhuber et al., 1987). A distorted helix is energetically unfavourably and often caused by the existence of the proline residue as the cyclic structure of the side chain limits the conformational flexibility of the protein backbone (Piela et al., 1987). The complex structure of human IL-2 with its α, β and γc receptors revealed that helices A′ and B′ (see Fig. 3) and their neighbouring regions contribute the major
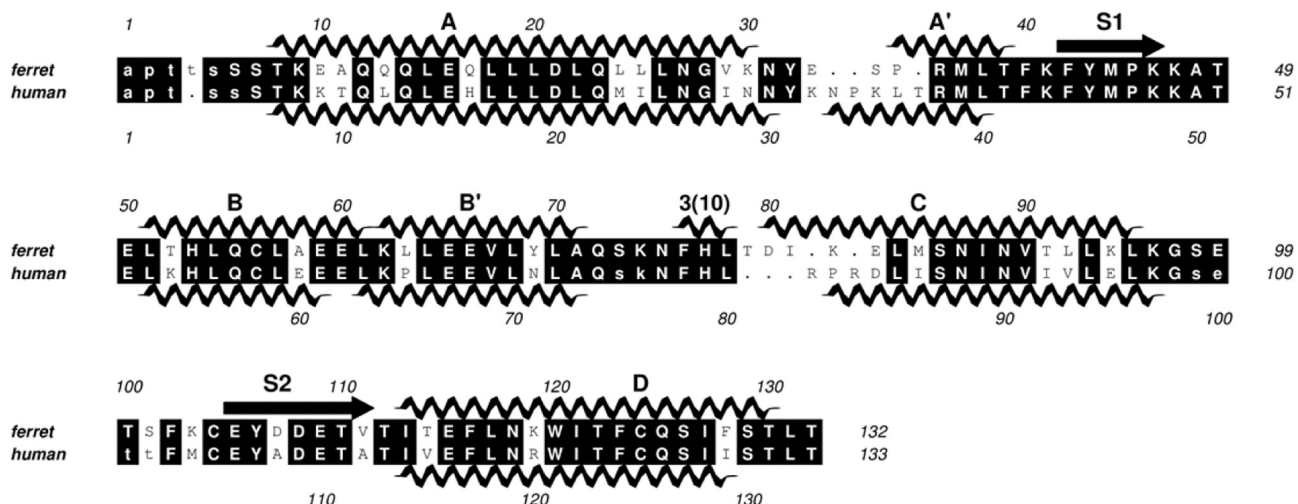

Fig. 3. Structure-based sequence alignment of ferret IL-2 molecule 2 with human IL-2. Alignment of the two molecules was performed with ALINE (Bond and Schuttelkopf, 2009).

interactions to form a "low affinity" complex with the alpha chain receptor as the first step of complex formation before the recruitment of the beta and gamma chains (Wang et al., 2005). The bound IL-2 structure in complex with the alpha chain receptor is very similar to that of its unbound state with only minor structural adaptations observed, including the partial unwinding of the first and last turn of helix A' and the last turn of helix B' (Bazan, 1992). The well-preserved overall structure suggests that human IL-2 maintains an active conformation even in the apo state, ready to forge binding interactions with the receptor. A similar structure is observed for ferret IL-2 molecule 1, indicating the conservation of these critical functional domains. In contrast, ferret IL-2 displays greater structural flexibility as shown by the conformational change in molecule 2, induced by an approaching molecule due to crystal packing. The movement of helices A' and B' in molecule 2 of ferret IL-2 may certainly disrupt the spatial arrangement of the residues involved in receptor binding interactions. It was shown in human IL-2 that residues Phe42, Tyr45 and Leu72 form critical hydrophobic interactions with the alpha chain receptor. Again, the corresponding residues are conserved in ferret IL-2 (Fig. 3), confirming their functional importance for engagement of the IL-2Rα, although their spatial positions are shifted in molecule 2 due to the movement of helices A' and B'. Structural alignment of ferret molecule 2 onto human IL-2 in the complex structure with the alpha chain receptor indicated that inter-atomic steric conflicts would occur between the straightened helix B' and the receptor.

Structure-based sequence alignments indicate that the proline residue (Pro65) responsible for the bent helix of human IL-2 is replaced by a leucine (Leu63) in ferret IL-2 (Fig. 3), and by a number of other residues (Asp, Ala) in other species. This replacement is probably the reason that leads to the increased conformational flexibility observed in the ferret IL-2 structure compared to the human IL2. This conformational flexibility may thus represent an intrinsic property of ferret IL-2 and structural adjustment can occur when induced by other molecules as shown above. While the bent helix may be necessary to maintain the receptor binding residues in the correct configuration, the varied structures suggest that unlike human IL-2, different states of the molecule may exist for ferret IL-2, which may implicate subtle differences between the two species IL-2's when initiating their biological functions.

3.3. Functional activity

To assess whether the ferret recombinant IL-2 was biologically functional, we tested if ferret LN cells sub-optimally stimulated with Con A could respond in a dose-dependent manner to ferret Il-2 through increased proliferation. Using the monomeric IL-2 isoform, we observed that concentrations from 0.05 ng/mL – 100 ng/mL showed significant increases in proliferation (p < 0.05 or greater) when compared Con A alone controls (Fig. 4A). Both the ferret IL-2 monomer and dimer stimulated the proliferation of a mouse cytotoxic T lymphocyte cell line (CTLL-2) in a dose-dependent manner (data not shown). The ferret IL-2 monomer and dimer appeared as effective as each other in this assay, but less effective than human IL-2.

Stimulation of naïve lymphocytes with IL-2 in culture induces expression of IFN-γ and Granzyme A mRNAs, mainly from CD8^{+} T cells (Janas et al., 2005). We have previously shown that ferret lymphocytes respond to mitogens and produce similar cytokines and chemokines as mouse and human cells (Carolan et al., 2014), thus we assessed whether recombinant ferret IL-2 proteins could stimulate ferret lymphocytes *in vitro*. Dose-dependent induction of mRNAs for the immune mediators, Granzyme A (Fig. 4B) and IFN-γ (Fig. 4C), was observed when ferret LN cells were cultured with ferret and human recombinant IL-2. Cells cultured with the ferret
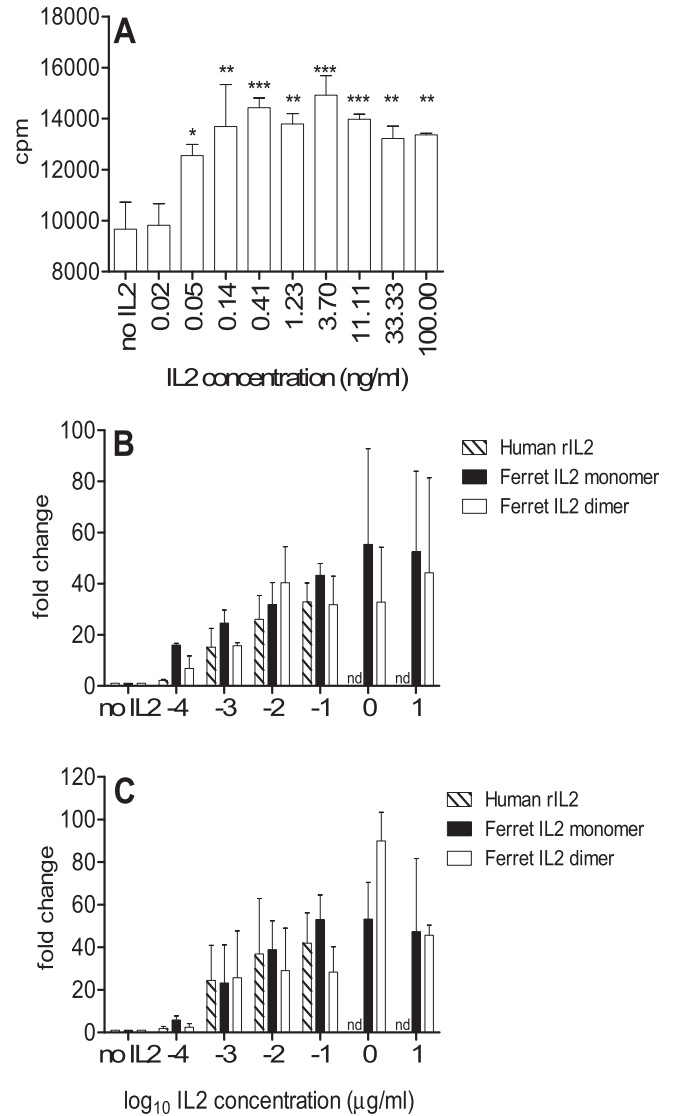

Fig. 4. Cellular responsiveness to ferret recombinant IL-2. (A) Ferret LN cells were suboptimally stimulated with Con A in the absence or presence of increasing doses of ferret recombinant IL-2 monomer. Proliferative responses were measured by the incorporation of ^{3}H-thymidine. The graph displays mean ± SE from three independent biological samples in triplicate and is representative of two independent experiments. P values: *<0.05, **<0.01, ***<0.001 (B, C) Expression of Granzyme A (B) or IFN-γ (C) mRNA in ferret LN cell cultures were detected by real time PCR assays. nd indicates not done.

IL-2 monomer produced the highest levels of the immune mediators, with a plateau at 1 and 10 μg/ml, respectively (Fig. 4B and C). The recombinant ferret proteins were not detected by ELISAs specific for mouse or human IL-2 (data not shown). This is a particularly relevant observation in the context of the aims of the present study; ferret IL-2 shares varying degrees of homology with the corresponding human (74.8% amino acid identity) and mouse (58.6%) proteins, as demonstrated by the observed structural variations in the case of the human and ferret alignment. While there may be a high degree of functional redundancy between these species with respect to *in vitro* assays, this does not extend to immunological cross-reactivity, at least in the kits tested in this study. This highlights the need to develop ferret-specific antibody reagents, not only for IL-2 but also for the broader suite of cytokines and lymphocyte cell-surface markers, in order to fully realise the value of the ferret as the most appropriate animal model for

enhancing our understanding of the immunobiology of the host response following infection with a number of lethal, human viral pathogens, including influenza.

Acknowledgements

References

Adams, P.D., Afonine, P.V., Bunkoczi, G., Chen, V.B., Davis, I.W., Echols, N., Headd, J.J., Hung, L.W., Kapral, G.J., Grosse-Kunstleve, R.W., McCoy, A.J., Moriarty, N.W., Oeffner, R., Read, R.J., Richardson, D.C., Richardson, J.S., Terwilliger, T.C., Zwart, P.H., 2010. PHENIX: a comprehensive Python-based system for macromolecular structure solution. Acta Crystallogr. D. Biol. Crystallogr. 66, 213—221.

Almeida, A.R., Legrand, N., Papiernik, M., Freitas, A.A., 2002. Homeostasis of peripheral CD4+ T cells: IL-2R alpha and IL-2 shape a population of regulatory cells that controls CD4+ T cell numbers. J. Immunol. 169, 4850—4860.

Arkin, M.R., Randal, M., DeLano, W.L., Hyde, J., Luong, T.N., Oslob, J.D., Raphael, D.R., Taylor, L., Wang, J., McDowell, R.S., Wells, J.A., Braisted, A.C., 2003. Binding of small molecules to an adaptive protein-protein interface. Proc. Natl. Acad. Sci. U. S. A. 100, 1603—1608.

Bazan, J.F., 1992. Unraveling the structure of IL-2. Science 257, 410—413.

Bond, C.S., Schuttelkopf, A.W., 2009. ALINE: a WYSIWYG protein-sequence alignment editor for publication-quality alignments. Acta Crystallogr. D. Biol. Crystallogr. 65, 510—512.

Bossart, K.N., Zhu, Z., Middleton, D., Klippel, J., Crameri, G., Bingham, J., McEachern, J.A., Green, D., Hancock, T.J., Chan, Y.P., Hickey, A.C., Dimitrov, D.S., Wang, L.F., Broder, C.C., 2009. A neutralizing human monoclonal antibody protects against lethal disease in a new ferret model of acute nipah virus infection. PLoS Pathog. 5, e1000642.

Boyman, O., Kovar, M., Rubinstein, M.P., Surh, C.D., Sprent, J., 2006. Selective stimulation of T cell subsets with antibody-cytokine immune complexes. Science 311, 1924—1927.

Boyman, O., Sprent, J., 2012. The role of interleukin-2 during homeostasis and activation of the immune system. Nat. Rev. Immunol. 12, 180—190.

Brandhuber, B.J., Boone, T., Kenney, W.C., McKay, D.B., 1987. Three-dimensional structure of interleukin-2. Science 238, 1707—1709.

Cameron, M.J., Kelvin, A.A., Leon, A.J., Cameron, C.M., Ran, L., Xu, L., Chu, Y.K., Danesh, A., Fang, Y., Li, Q., Anderson, A., Couch, R.C., Paquette, S.G., Fomukong, N.G., Kistner, O., Lauchart, M., Rowe, T., Harrod, K.S., Jonsson, C.B., Kelvin, D.J., 2012. Lack of innate interferon responses during SARS coronavirus infection in a vaccination and reinfection ferret model. PLoS One 7, e45842.

Carolan, L.A., Butler, J., Rockman, S., Guarnaccia, T., Hurt, A.C., Reading, P., Kelso, A., Barr, I., Laurie, K.L., 2014. TaqMan real time RT-PCR assays for detecting ferret innate and adaptive immune responses. J. Virol. Methods 205C, 38—52.

Cousens, L.P., Orange, J.S., Biron, C.A., 1995. Endogenous IL-2 contributes to T cell expansion and IFN-gamma production during lymphocytic choriomeningitis virus infection. J. Immunol. 155, 5690—5699.

D'Souza, W.N., Lefrancois, L., 2003. IL-2 is not required for the initiation of CD8 T cell cycling but sustains expansion. J. Immunol. 171, 5727—5735.

Emsley, P., Lohkamp, B., Scott, W.G., Cowtan, K., 2010. Features and development of Coot. Acta Crystallogr. D. Biol. Crystallogr. 66, 486—501.

Evans, P., 2006. Scaling and assessment of data quality. Acta Crystallogr. D. Biol. Crystallogr. 62, 72082.

Janas, M.L., Groves, P., Kienzle, N., Kelso, A., 2005. IL-2 regulates perforin and granzyme gene expression in CD8+ T cells independently of its effects on survival and proliferation. J. Immunol. 175, 8003—8010.

Kabsch, W., 2010. Xds. Acta Crystallogr. D. Biol. Crystallogr. 66, 125—132.

Kundig, T.M., Schorle, H., Bachmann, M.F., Hengartner, H., Zinkernagel, R.M., Horak, I., 1993. Immune responses in interleukin-2-deficient mice. Science 262, 1059—1061.

Malek, T.R., Castro, I., 2010. Interleukin-2 receptor signaling: at the interface between tolerance and immunity. Immunity 33, 153—165.

Malek, T.R., Yu, A., Vincek, V., Scibelli, P., Kong, L., 2002. CD4 regulatory T cells prevent lethal autoimmunity in IL-2Rbeta-deficient mice. Implications for the nonredundant function of IL-2. Immunity 17, 167—178.

McCoy, A.J., Grosse-Kunstleve, R.W., Adams, P.D., Winn, M.D., Storoni, L.C., Read, R.J., 2007. Phaser crystallographic software. J. Appl. Crystallogr. 40, 658—674.

Mott, H.R., Campbell, I.D., 1995. Four-helix bundle growth factors and their receptors: protein-protein interactions. Curr. Opin. Struct. Biol. 5, 114—121.

Music, N., Reber, A.J., Lipatov, A.S., Kamal, R.P., Blanchfield, K., Wilson, J.R., Donis, R.O., Katz, J.M., York, I.A., 2014. Influenza vaccination accelerates recovery of ferrets from lymphopenia. PLoS One 9, e100926.

Pallister, J., Middleton, D., Wang, L.F., Klein, R., Haining, J., Robinson, R., Yamada, M., White, J., Payne, J., Feng, Y.R., Chan, Y.P., Broder, C.C., 2011. A recombinant Hendra virus G glycoprotein-based subunit vaccine protects ferrets from lethal Hendra virus challenge. Vaccine 29, 5623—5630.

Papiernik, M., de Moraes, M.L., Pontoux, C., Vasseur, F., Penit, C., 1998. Regulatory CD4 T cells: expression of IL-2R alpha chain, resistance to clonal deletion and IL-2 dependency. Int. Immunol. 10, 371—378.

Peng, X., Alfoldi, J., Gori, K., Eisfeld, A.J., Tyler, S.R., Tisoncik-Go, J., Brawand, D., Law, G.L., Skunca, N., Hatta, M., Gasper, D.J., Kelly, S.M., Chang, J., Thomas, M.J., Johnson, J., Berlin, A.M., Lara, M., Russell, P., Swofford, R., Turner-Maier, J., Young, S., Hourlier, T., Aken, B., Searle, S., Sun, X., Yi, Y., Suresh, M., Tumpey, T.M., Siepel, A., Wisely, S.M., Dessimoz, C., Kawaoka, Y., Birren, B.W., Lindblad-Toh, K., Di Palma, F., Engelhardt, J.F., Palermo, R.E., Katze, M.G., 2014. The draft genome sequence of the ferret (Mustela putorius furo) facilitates study of human respiratory disease. Nat. Biotechnol. 32, 1250—1255.

Piela, L., Nemethy, G., Scheraga, H.A., 1987. Proline-induced constraints in alpha-helices. Biopolymers 26, 1587—1600.

Rickert, M., Wang, X., Boulanger, M.J., Goriatcheva, N., Garcia, K.C., 2005. The structure of interleukin-2 complexed with its alpha receptor. Science 308, 1477—1480.

Sadlack, B., Lohler, J., Schorle, H., Klebb, G., Haber, H., Sickel, E., Noelle, R.J., Horak, I., 1995. Generalized autoimmune disease in interleukin-2-deficient mice is triggered by an uncontrolled activation and proliferation of CD4+ T cells. Eur. J. Immunol. 25, 3053—3059.

Sadlack, B., Merz, H., Schorle, H., Schimpl, A., Feller, A.C., Horak, I., 1993. Ulcerative colitis-like disease in mice with a disrupted interleukin-2 gene. Cell 75, 253—261.

Schorle, H., Holtschke, T., Hunig, T., Schimpl, A., Horak, I., 1991. Development and function of T cells in mice rendered interleukin-2 deficient by gene targeting. Nature 352, 621—624.

Stauber, D.J., Debler, E.W., Horton, P.A., Smith, K.A., Wilson, I.A., 2006. Crystal structure of the IL-2 signaling complex: paradigm for a heterotrimeric cytokine receptor. Proc. Natl. Acad. Sci. U. S. A. 103, 2788—2793.

Tom, R., Bisson, L., Durocher, Y., 2008. Transfection of HEK293-EBNA1 cells in suspension with linear PEI for production of recombinant proteins. CSH Protoc. 2008 pdb prot4977.

Wang, X., Rickert, M., Garcia, K.C., 2005. Structure of the quaternary complex of interleukin-2 with its alpha, beta, and gammac receptors. Science 310, 1159—1163.

Willerford, D.M., Chen, J., Ferry, J.A., Davidson, L., Ma, A., Alt, F.W., 1995. Interleukin-2 receptor alpha chain regulates the size and content of the peripheral lymphoid compartment. Immunity 3, 521—530.

Williams, M.A., Tyznik, A.J., Bevan, M.J., 2006. Interleukin-2 signals during priming are required for secondary expansion of CD8+ memory T cells. Nature 441, 890—893.

Winn, M.D., Ballard, C.C., Cowtan, K.D., Dodson, E.J., Emsley, P., Evans, P.R., Keegan, R.M., Krissinel, E.B., Leslie, A.G., McCoy, A., McNicholas, S.J., Murshudov, G.N., Pannu, N.S., Potterton, E.A., Powell, H.R., Read, R.J., Vagin, A., Wilson, K.S., 2011. Overview of the CCP4 suite and current developments. Acta Crystallogr. D. Biol. Crystallogr. 67, 235—242.